ResearchGate

See discussions, stats, and author profiles for this publication at: https://www.researchgate.net/publication/229871274

Polaron stability under collision with different defects in conjugated polymers

ARTICLE *in* INTERNATIONAL JOURNAL OF QUANTUM CHEMISTRY · NOVEMBER 2006

Impact Factor: 1.43 · DOI: 10.1002/qua.21012

CITATIONS
4

READS
15

2 AUTHORS:

Matheus P. Lima
Universidade Federal de São Carlos
21 PUBLICATIONS **112** CITATIONS
SEE PROFILE

Geraldo Magela e Silva
University of Brasília
90 PUBLICATIONS **509** CITATIONS
SEE PROFILE

Available from: Geraldo Magela e Silva
Retrieved on: 26 January 2016

WILEY InterScience® DISCOVER SOMETHING GREAT

Polaron Stability Under Collision With Different Defects in Conjugated Polymers

MATHEUS PAES LIMA, GERALDO MAGELA E SILVA

Institute of Physics, University of Brasíla, 70.917-970, Brasília, Distrito Federal, Brazil

Received 13 December 2005; accepted 21 February 2006
Published online 17 April 2006 in Wiley InterScience (www.interscience.wiley.com).
DOI 10.1002/qua.21012

ABSTRACT: Polarons are charge carriers generated by doping or photo-excitation in conjugated polymers. The dynamics of polaron–soliton and polaron–bipolaron collisions in conjugated polymers is numerically studied using the Su–Schrieffer–Heeger model extended to include an external electric field, Coulomb interactions, and impurities interactions. The time-dependent unrestricted Hartree–Fock approximation is considered. The stability of polarons determines whether the charge transport by these structural defects are modified under these collisions. An energetic analysis determines whether the energy levels associated with solitons, polarons, and bipolarons change with collisions. We show that these structural defects have great stability in collisions. The bipolaron mobility does not change under polaron–bipolaron collisions. In contrast, we find that there is a great exchange of linear momentum in the collisions between solitons and polarons.
© 2006 Wiley Periodicals, Inc. Int J Quantum Chem 106: 2603–2608, 2006

Key words: soliton; polaron; bipolaron

Introduction

In conjugated polymers, optical and electrical properties can be changed by doping or photo-excitation [1–3]. These special properties, combined with the mechanical properties of a plastic, offer great possibilities in technological applications. Chemical and biological sensors, transistors, integrated circuits, light-emitting diodes (LEDs), and solar cells are some of the devices based on conducting polymers [4–9]. These organic polymers are the focus of current research [10–12].

The mechanism of charge transport in conjugated polymers is based on the presence of nonlinear excitations, such as solitons, polarons, and bipolarons, which are generated by doping or photo-excitation. These defects are specific deformations that range few sites in polymeric chain and that can have charge and spin. An external electromagnetic field can move these defects through the chain. The study of the properties of these defects is in the basis of that new research [13–18].

Correspondence to: M. P. Lima; e-mail: matheus@fis.unb.br

© 2006 Wiley Periodicals, Inc.

Solitons can be neutral with spin $\pm 1/2$, or they can be charged, with $Q = \pm e$ and no spin. Polarons have charge $Q = \pm e$ with spin $\pm 1/2$, responding to magnetic and electric fields simultaneously. Bipolarons have charge $Q = \pm 2e$ and have no spin. In association with these defects, electronic levels appear inside the gap.

Some studies have shown that polaron defects have great instability under the application of a strong external electric field [14, 19]. It can also be observed that in the polaron motion, the polaron structure becomes blurred after being subjected to lengthy simulations. Polarons function as charge carriers, and the instability of these structural defects is closely related to the electric and the optical properties of conjugated polymers.

In the present work we investigate numerically the stability of polarons in polaron–soliton and polaron–bipolaron collisions in conjugated polymers. We use a Su–Schrieffer–Heeger (SSH) model, modified to include an external electric field and electron–electron interactions via a Parr–Pariser–Pople (PPP) mean field Hamiltonian and site-type impurity interactions. Within the unrestricted Hartree–Fock (UHF) approximation, we study the dynamics using the Euler–Lagrange equations to describe the nuclear time evolution, and the Schrödinger equation to describe the time evolution of the electronic part.

Solitons are present in symmetric chains (*trans*-polyacetylene), while bipolarons are present in asymmetric chains (e.g., *cis*-polyacetylene, polythiophene, polypyrrol). A Brazovskii–Kirova (BK) symmetry-breaking interaction term was used in the SSH model to study the asymmetric (nondegenerate ground-state) chains [20].

Model

The Hamiltonian is the SSH Hamiltonian extended to include an external electric field, combined with PPP terms, with BK-symmetry interactions and site-type impurity terms:

$$H(t) = -\sum_{i,s}(t_{i,i+1}C^{\dagger}_{i+1,s}C_{i,s} + H.c.) + U\sum_i\left(n_{i\uparrow} - \frac{1}{2}\right) \times \left(n_{i\downarrow} - \frac{1}{2}\right) + V\sum_i (n_i - 1)(n_{i+1} - 1) + \sum_i \frac{K}{2}y_i^2 + \sum_i \frac{M}{2}\dot{u}_i^2 + \sum_{p,s} V_p C^{\dagger}_{p,s}C_{p,s}, \quad (1)$$

where $C^{\dagger}_{i,s}(C_{i,s})$ is the creation (annihilation) operator of a π electron with spin s at the ith lattice site, $n_{i,s} \equiv C^{\dagger}_{i,s}C_{i,s}$ is the number operator, and $n_i = \Sigma_s n_{i,s}$. $y_n \equiv u_{n+1} - u_n$, where u_n is the displacement of nth CH group from equilibrium position in the undimerized phase. $t_{n,n+1} = \exp(-i\gamma A)[(1 + (-1)^n\delta_0)t_0 - \alpha y_n]$, t_0 is the transfer integral between the nearest-neighbor sites in the undimerized chains, α is the electron–phonon coupling, and δ_0 is the BK symmetry-breaking parameter. M is the mass of a CH group, K is the spring constant of a σ-bond, and U and V are the on-site and nearest-neighbor Coulomb repulsion strengths, respectively. V_p is the strength of an impurity located at the pth site, $\gamma \equiv ea/(\hbar c)$, where e is the absolute value of the electronic charge, a is the lattice constant, and c is the light velocity. The relationship between the time-dependent vector potential A and the uniform electric field E is given by $E = -(1/c)$ Å. We use as parameters the commonly accepted values for conjugated polymers: $t_0 = 2.5$ eV, $K = 21$ eV Å^{-2}, $\alpha = 4.1$ eV Å^{-1}, $U = t_0/2$, $V = U/2$, $a = 1.22$ Å [3], and a bare optical phonon energy $\hbar\omega_Q = \sqrt{4K/M} = 0.16$ eV.

To perform the time evolution of the system, first, within the UHF approximation, we prepare a stationary state, which is fully self-consistent with the degrees of freedom of electrons and phonons. Then we perform the time evolution by considering the time-dependent unrestricted Hartree–Fock (TD UHF) approximation, and find the following equation for one-particle wave functions:

$$i\hbar\dot{\psi}_{k,s}(i,t) = -[t^*_{i,i+1} + V\tau_s(i,t)]\psi_{k,s}(i+1,t) - [t_{i-1,i} + V\tau^*_s(i-1,t)]\psi_{k,s}(i-1,t) + \left\{U\left[\rho_{-s}(i,t) - \frac{1}{2}\right] + \sum_p V_p\delta_{i,p} + V\sum_{s'}[\rho_{s'}(i+1,t) + \rho_{s'}(i-1,t) - 1]\right\} \times \psi_{k,s}(i,t) \quad (2)$$

with

$$\rho_s(i,t) = \sum_k{}' \psi^*_{k,s}(i,t)\psi_{k,s}(i,t)$$

$$\tau_s(i,t) = \sum_k{}' \psi^*_{k,s}(i+1,t)\psi_{k,s}(i,t). \quad (3)$$

The equations for the above one-particle wave functions are solved coupled to the Euler–Lagrange

equations, which are used to perform the CH site motion dynamics. The Euler–Lagrange equations are given by

$$\frac{d}{dt}\left(\frac{\partial\langle L\rangle}{\partial \dot{w}_n}\right) - \frac{\partial\langle L\rangle}{\partial w_n} = 0, \quad (4)$$

where

$$\langle L\rangle = \langle T\rangle - \langle V\rangle. \quad (5)$$

We obtain

$$M\ddot{u}_n = F_n(t), \quad (6)$$

where

$$F_n(t) = -K[2u_n(t) - u_{n+1}(t) - u_{n-1}(t)] + \alpha[e^{i\gamma A(t)}(B_{n,n+1} - B_{n-1,n}) + e^{-i\gamma A(t)}(B_{n+1,n} - B_{n,n-1})], \quad (7)$$

where $B_{n,n'} \equiv \sum_{k,s}{}' \psi^*_{k,s}(n, t)\psi_{k,s}(n', t)$. The prime on the summation means that the sum is taken over the occupied single-particle states in the initial stationary state. Equations (2) and (6) perform the electronic and nuclear dynamics, respectively.

These equations of motion are solved by discretizing the time variable with a step Δt. The time step Δt is chosen so that the change in $u_i(t)$ and $A(t)$ during this interval is always very small in the electronic scale.

Equation (2) is integrated by introducing single-electron eigenstates at each moment. Therefore, the solutions of the time-dependent Hartree–Fock equations can then be put in the form

$$\psi_{k,s}(n, t_{j+1}) = \sum_l \left[\sum_m \phi^*_{l,s}(m, t_j)\psi_{k,s}(m, t_j)\right] \times e^{-i(\epsilon_l \Delta t/\hbar)}\phi_{l,s}(n, t_j), \quad (8)$$

where $\{\phi_l\}$ and $\{\epsilon_l\}$ are the eigenfunctions and the eigenvalues of the single-electron equations at a given time t_j.

The lattice equations are written as

$$u_i(t_{j+1}) = u_i(t_j) + \dot{u}_i(t_j)\Delta t \quad (9)$$

$$\dot{u}_i(t_j + 1) = \dot{u}_i(t_j) + \frac{F_i(t_j)}{M}\Delta t. \quad (10)$$

Hence, the electronic wave functions and the displacement coordinates at $j + 1$th time step are obtained from the jth time step.

Periodic boundary conditions are assumed for the electronic wave functions, $\psi_{k,s}$, and the lattice displacement, u_i.

The position, energy, and charge are observed every 1,000 time steps. A fixed time step of $\Delta t = 0.004$ femtosecond (fs) is used. We follow the dynamics of the system up to 440 fs. The numerical stability and reliability of the simulations are established by the conservation of the total energy of the system when the electric field is switched off.

Results of Simulations

We perform the simulations by varying the electric field. We begin with a fully self-consistent state that contains one soliton and one polaron in the polaron–soliton collisions, and one polaron and one bipolaron in the polaron–bipolaron collisions. To study chains doped with donor impurities, we consider all the defects positively charged. An external electric field is used to accelerate the defects, to perform the collisions. This electric field is turned on in the beginning of the simulations and turned off after 60 fs. Its intensity ranges from $|E| = 6 \times 10^4 V/m$ to $|E| = 1.3 \times 10^5 V/m$, and it is switched on and off adiabatically [21]. An external electric field of $>1.3 \times 10^5 V/m$ could change the polaron characteristics [14]. Because these structural defects can be attracted or repelled by impurities, we have doped the chain to manipulate the initial position of the soliton, polaron, and bipolaron.

An order parameter $\bar{y}_i$ is used to analyze the simulations:

$$\bar{y}_i = (-1)^i \frac{(-y_{i-1} + 2y_i - y_{i+1})}{4}.$$

POLARON–SOLITON COLLISIONS

We consider polymer chains with $N = 107$ sites. We found that the polaron and the soliton respond similarly upon the action of an external electric field, running along the chain with similar velocities. Therefore, to perform the collision, the addition of impurities is necessary.

Figure 1 shows the order parameter of a collision between a soliton and a polaron. A donor impurity with the impurity strength $V_p = 0.18t_0$ was added

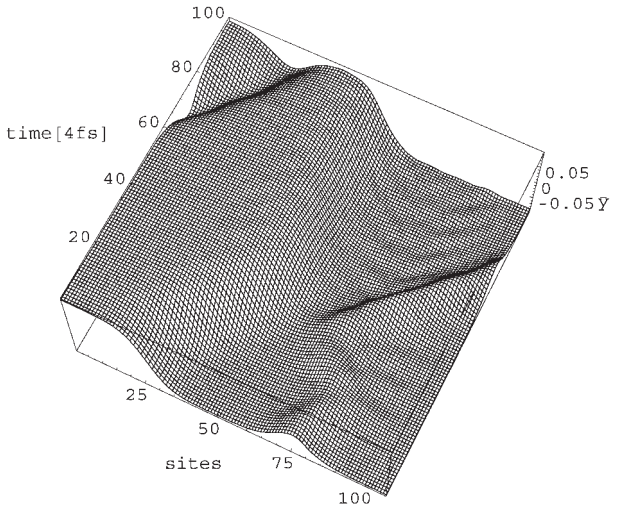

FIGURE 1. Order parameter of a soliton–polaron collision. $|E| = 1.04 \times 10^4 V/m$; $V_p = 0.18t_0$.

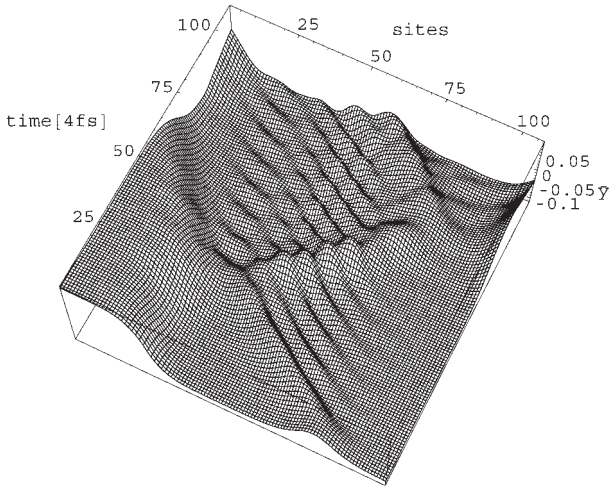

FIGURE 2. Order parameter of a soliton–polaron collision. $|E| = 1.04 \times 10^4 V/m$; $V_p = 0.15t_0$.

near the polaron position in order to trap the polaron. The soliton remains free to run along to the chain when the external electric field is applied. In this simulation we apply an electric field with $|E| = 1.04 \times 10^4 V/m$. The impurity is removed before the collision, so that only the effects due to the collision are observed.

A great transfer of linear momentum can be seen in the order parameter time evolution (Fig. 1). The soliton collides with the polaron and, due to the collision, the soliton transfers a great percentage of its translational energy to the polaron. In this specific case, the collision is quasi-elastic.

Figure 2 uses an impurity with $V_p = 0.15t_0$ to keep trapped the soliton, while the polaron is free to move. $|E| = 1.04 \times 10^4 V/m$. In this collision, there is again a great transfer of linear momentum. It can be observed that the polaron was reflected by the soliton and that the soliton received translational energy from the polaron.

We performed several simulations of this type of collision. We changed the electric field used to accelerate the defects, the impurity location, and the impurity strength V_p. In all collisions, we observe the transfer of translational energy between the polaron and the soliton. Analysis of the simulations shows that the polaron has a smaller effective mass compared with solitons.

The general characteristics of these defects do not change under this type of collision. The order parameter shows that a soliton and a polaron are not destroyed by the collision. Analysis of the energy levels in a soliton–polaron collision shows that the energy levels associated with the defects do not feel any collision effects (Fig. 3). This result is the same in all the polaron–soliton collisions that we made. Therefore, the simulations of the collisions between polarons and solitons demonstrate that the defects are not destroyed under this type of collision. There is a great transfer of translational energy, and the polaron motion is more modified than the soliton motion under collision.

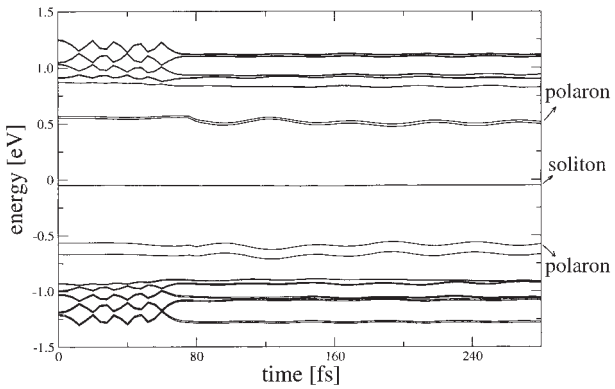

FIGURE 3. Levels of energy near of the gap in a soliton–polaron collision. In this case, an impurity with $V_p = 0.015t_0$ is used to keep trapped the polaron close to its initial position. The external electron field with $|E| = 1.04 \times 10^4 V/m$ is used to accelerate the soliton.

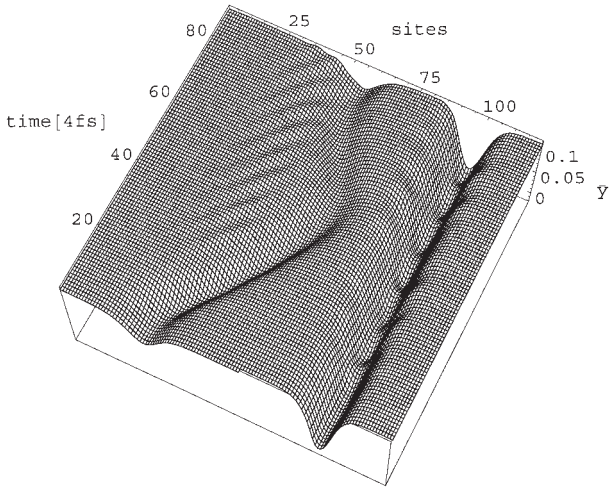

FIGURE 4. Order parameter of a polaron–bipolaron collision. $|E| = 1.04 \times 10^4 V/m$.

POLARON–BIPOLARON COLLISIONS

To perform the polaron–bipolaron collisions, we use a chain with $N = 104$ sites. The BK-parameter is considered in the Hamiltonian to study asymmetric chains. WE use $\delta_0 = 0.05$.

Figure 4 represents the time evolution surface of the order parameter of a collision between a polaron and a bipolaron. A donor impurity with $V_p = 0.15t_0$ is added near the bipolaron position to keep it trapped close to its initial position. This impurity was removed after 68 fs from the beginning of the simulation. It can be observed that the bipolaron does not feel any effect due to this collision, while the polaron is reflected by the bipolaron. This shows that the effective mass of a bipolaron is very greater than the effective mass of a polaron. In Figure 4, it can also be seen that the polaron has great stability under this collision. The energy levels located in the gap in Figure 5 observed to be associated with the defects do not feel any effect related to the collision.

In contrast, when a bipolaron collides with a stopped polaron, the bipolaron motion is practically unchanged and the polaron is scattered, moving freely after the collision.

We have performed several simulations of polaron–bipolaron collisions by varying the electric field, and changing the impurity location and its strength V_p. Analyzing all simulations, we can conclude that neither the polaron structure nor the bipolaron structure is destroyed under this type of collision. Analysis of the levels of energy located in the gap indicates that the polaron–bipolaron collision causes changes only in the mean free path of the polaron, thus affecting its mobility.

Conclusions

Using a modified SSH model that includes the action of an external electric field, Coulomb interactions, and impurity interactions, we studied the stability of polarons in polaron–solitons and polaron–bipolaron collisions in conjugated polymers. Within the UHF approximation, we performed the time evolution from an initial fully self-consistent state, using the Euler–Lagrange equations to the nuclear part and the Schrödinger equation to the electronic part.

In polaron–soliton collisions we have found that there is a greater transfer of translational energy between polarons and solitons, but the polaron changes its velocity more easily than the soliton. This shows that the effective mass of polarons is smaller than the effective mass of solitons. However, the masses of polaron and solitons have the same order of magnitude. These defects do not overlap during the collisions. The main characteristics, such as the bond structure and energy levels inside the gap associated with them, remain the same. The fact that the defects are not destroyed shows that, in polyacetylene, the collisions between different defects do not hinder the charge transport by solitons and polarons. Despite the fact that the polarons are more instable than solitons, the collisions between solitons and polarons are not a factor of instability for polarons.

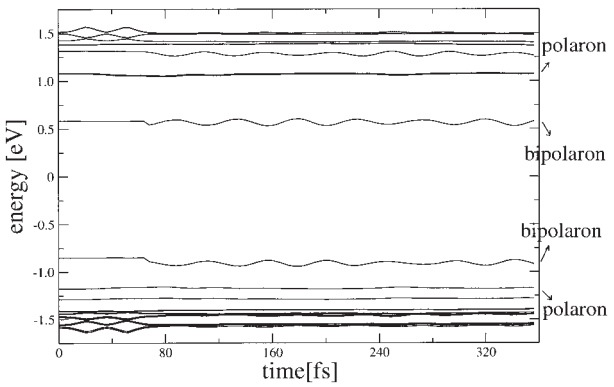

FIGURE 5. Levels of energy near the gap in a polaron–bipolaron collision.

The study of collisions between polarons and bipolarons shows that these defects do not overlap during the collisions in the same way as polaron–soliton collisions. These simulations show that the bipolaron mobility does not change under polaron–bipolaron collisions. The presence of bipolarons in the polymer limits the movement of polarons, because the polarons cannot cross the bipolaron, such that in conjugated polymers holding bipolarons, the polaron mobility is compromised. Therefore, their function as charge carriers should be considered with care.

Our general analysis of collisions with different defects in conjugated polymers shows that the polaron defects are not destroyed in these collisions and, compared with solitons and bipolarons, the polaron is the more movable defect. Additionally, these collisions do not change the configuration of the energy levels. Therefore, collisions affect conduction by changing the mobility of the charge carriers.

References

1. Heeger, A. J. J Phys Chem B 2001, 105, 8475.
2. Shirakawa, H.; Ikeda, S. Polymer J 1971, 2, 231.
3. Chiang, C. K.; Fincher, C. R., Jr.; Park, V. W.; Heeger, A. J.; Shirakawa, H.; Louis, E. J.; Gau, S. C.; MacDiarmid, A. G. Phys Rev Lett 1977, 39, 1098.
4. Janata, J.; Josowicz, M. Nat Mater 2003, 2, 19.
5. Li, G.; Martinez, C.; Semancik, S. J Am Chem Soc 2005, 127, 4903.
6. Gerard, M.; Chaubey, A.; Malhotra, B. D. Biosens Bioelectron 2002, 17, 345.
7. Gurunathan, K.; Murugan, A. V.; Marimuthu, R.; Mulik, U. P.; Amalnerkar, D. P. Mater Chem Phys 1999, 61, 173.
8. Angelopoulos, M. IBM J Res Dev 2001, 45, 57.
9. Spanggaard, H.; Krebs, F. C. Sol Energy Mater 2004, 83, 125.
10. Naarmann, H.; Theophilou, N. Synth Met 1987, 22, 1.
11. McCullogh, R. D.; Williams, S. P. J Am Chem Soc 1993, 115, 11686.
12. McDiarmid, A. G. In Conjugated Polymers and Related Materials: The Interconnection of Chemical and Electronic Structure; Salaneck, W. R.; Lundstrm, I.; Rånby, B., editors; Oxford Scientific: Oxford, UK, 1993; p 285.
13. Pinheiro, C. S.; e Silva, G. M. Theochem 1997, 394, 161.
14. e Silva, G. M. Phys Rev B 2000, 61, 10777.
15. Onodera, Y.; Okuno, S. J Phys Soc Jpn 1982, 52, 2478.
16. Pinheiro, C. S.; Acioli, P. H.; e Silva, G. M. Theochem 2001, 539, 55.
17. Streitwolf, H. W. Phys Rev B 1998, 58, 14356.
18. Johansson, A.; Stafström, S. Phys Rev Lett 2001, 86, 3602.
19. Yan, Y. H.; An, Z.; Wu, C. Q. Eur Phys J B 2004, 42, 157.
20. Brazovskii, S. A.; Kirova, N. N., Pis'ma Z. Eksp Teor Fiz 1981, 33, 6 (JETP Lett. 1981, 33, 4).
21. Kuwabara, M.; Ono, Y.; Terai, A. J Phys Soc Jpn 1991, 60, 1286.